10. A. Stöhr, A. Akrout, R. Buß, B. Charbonnier, F. van Dijk, A. Enard, S. Fedderwitz, D. Jäger, M. Huchard, F. Lecoche, J. Marti, R. Sambaraju, A. Steffan, A. Umbach, and M. Weiß, "60 GHz radio-over-fiber technologies for broadband wireless services," J. Opt. Netw. **8**(5), 471–487 (2009).
11. L. Zhang, X. Hu, P. Cao, and Y. Su, "A 60-GHz RoF system in WDM-PON with reduced number of modulators and low-cost electronics," in *2010 Photonics Global Conference (PGC)* (IEEE, 2010), paper conf10a420.
12. C. H. Yeh and C. W. Chow, "Heterogeneous radio-over-fiber passive access network architecture to mitigate Rayleigh backscattering interferometric beat noise," Opt. Express **19**(7), 5735–5740 (2011).
13. Q. Chang, T. Ye, J. Gao, and Y. Su, "Generation of 60-GHz optical millimeter-wave and 20-GHz channel-spaced optical multicarrier using two cascade 10-GHz modulators," in *Asia Optical Fiber Communication and Optoelectronic Exposition and Conference*, OSA Technical Digest (CD) (Optical Society of America, 2008), paper SaJ1.
14. Q. Chang, Y. Tian, J. Gao, T. Ye, Q. Li, and Y. Su, "Generation and transmission of optical carrier suppressed-optical differential (Qudrature) phase-shift keying (OCS-OD(Q)PSK) signals in radio over fiber systems," J. Lightwave Technol. **26**(15), 2611–2618 (2008).
15. L. Zhang, Y. Wu, X. Hu, T. Wang, P. Cao, and Y. Su, "Simultaneous transmission of three services in a WDM-PON system with wireless access for multicast data," in *2010 Asia Communications and Photonics Conference and Exhibition (ACP)* (2010), pp. 443–444.

1. Introduction

Next-generation access networks require large bandwidths and high data rates in both wired and wireless accesses for the ever-increasing video-based interactive and multimedia services. It is desirable to simultaneously transmit baseband and radio-frequency (RF) signals in an integrated platform [1–3]. For wired access networks, wavelength division multiplexed–passive optical network (WDM-PON) is attractive for its advantages of high capacity, large coverage range, upgradeability, and cost-effective configurations [4]. With respect to wireless access networks, 60-GHz access system has gained much attention for its wide bandwidth availability over the 7-GHz unlicensed millimeter-wave (MMW) band [5, 6]. However, due to high atmospheric loss of the 60-GHz MMW signal, the access convergence is limited to tens of meters [6]. Thanks to the huge bandwidth and low transmission loss provided by optical fibers, radio-over-fiber (RoF) technology is considered to be a promising solution to increase capacity and mobility as well as to reduce overall cost in wireless access networks [7]. As a result, the WDM-PON-RoF converged system is believed to be a promising candidate to simultaneously provide wired and wireless services. In Ref. [8–10], a WDM-PON was integrated with a 60-GHz RoF system for providing multi-gigabit, integrated wired and wireless services. However, if the WDM-PON has N wavelength channels, more than 2N modulators would be needed in the optical line terminal/central station (OLT/CS) [8, 9]. In Ref. [10], 30-GHz synthesizer, electronic devices and modulators were used to up-convert the baseband signal. In our previous work, we proposed a scheme to integrate a WDM-PON with a 60-GHz RoF system [11], however, only a single-channel system was implemented, which cannot capitalize the advantage of the reduced number of modulators and the upgradeability to multi-channel system.

In this paper, we experimentally demonstrate a simple and cost-effective scheme to integrate a WDN-PON with a 60-GHz RoF system. Detailed operation principle and power budget are also investigated. Comparing with the previous reports [8–10, 12], our scheme has several advantages: firstly, one single-drive modulator is used to generate both optical carrier suppression (OCS) and based signals for wireless and wired applications, and only N + 1 single-drive modulators are required for N WDM channels using a new structure; besides, based on a new frequency-sextupling and optical carrier suppression-differential phase shift keying (OCS-DPSK) modulation technology, only 10-GHz electronic devices and modulators are needed for the generation of 60-GHz wireless signals [13]; additionally, bi-directional RoF system is achieved with independent wired, wireless and upstream data. At the optical network units/ base stations (ONUs/BSs), the downstream baseband DPSK signals are re-modulated by upstream data, therefore, the cost of the system is greatly reduced since no light sources and wavelengths management are required in the ONUs/BSs.

#167150 - $15.00 USD Received 20 Apr 2012; accepted 7 May 2012; published 15 Jun 2012
(C) 2012 OSA

2. Architecture and principle of operation

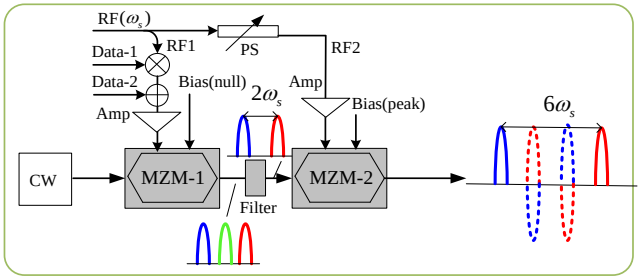

Fig. 1. Principle of the generation of OCS-DPSK signal with sixfold frequency.

Figure 1 shows the principle of the generation of OCS-DPSK signal with six-fold frequency. An RF clock S_{RF1} is mixed with an electrical data S_{D1} (Data-1) to generate an electrical subcarrier multiplexed (SCM) signal, which is then combined with another electrical data S_{D2} (Data-2). MZM-1 is driven by the combined signal together with the bias voltage, which can be expressed by: $V_1(t) = \varepsilon_1 V_\pi + \alpha_1 V_\pi D_1(t)\cos(\omega_s t) + \alpha_2 V_\pi D_2(t)$, where ω_s is the frequency of the RF clock. ε_1, α_1 and α_2 are the bias voltage of the modulator, and the driving amplitudes of the SCM signal and Data-2 normalized to the half-wave voltage V_π. $D_1(t)$ and $D_2(t)$ = [1 or −1] represent the input data.

According to Ref. [14], the field of the output of MZM-1 can be expressed by

$$E_{out1} = E_0 \cos(\omega_c t)\cos\{\frac{\pi}{2}[\varepsilon_1 + \alpha_1 D_1(t)\cos(\omega_s t) + \alpha_2 D_2(t)]\} \tag{1}$$

where E_0 and ω_c are the amplitude and the frequency of the input continual wave (CW) light, respectively. Since the MZM-1 is biased at the null of transmission curve (ε_1 = 1), we have

$$\begin{aligned} E_{out1} &= E_0 \cos(\omega_c t)\cos\{\frac{\pi}{2} + \frac{\pi}{2}[\alpha_1 D_1(t)\cos(\omega_s t) + \alpha_2 D_2(t)]\} \\ &= -E_0 \cos(\omega_c t)\sin\{\frac{\pi}{2}[\alpha_1 D_1(t)\cos(\omega_s t) + \alpha_2 D_2(t)]\} \\ &= -E_0 \cos(\omega_c t)\{\sin[\frac{\pi}{2}\alpha_1 D_1(t)\cos(\omega_s t)]\cos[\frac{\pi}{2}\alpha_2 D_2(t)] + \cos[\frac{\pi}{2}\alpha_1 D_1(t)\cos(\omega_s t)]\sin[\frac{\pi}{2}\alpha_2 D_2(t)]\} \end{aligned} \tag{2}$$

We expand the Eq. (2) using Bessel functions as

$$\begin{aligned} E_{out1} = -E_0 \cos(\omega_c t)\{&2\cos[\frac{\pi}{2}\alpha_2 D_2(t)]\times\sum_{n=1}^{\infty}(-1)^n J_{(2n-1)}[\frac{\pi}{2}\alpha_1 D_1(t)]\cos[(2n-1)\cdot\omega_s t] \\ &+ \sin[\frac{\pi}{2}\alpha_2 D_2(t)]\times\{J_0[\frac{\pi}{2}\alpha_1 D_1(t)] + 2\sum_{n=1}^{\infty}(-1)^n J_{2n}[\frac{\pi}{2}\alpha_1 D_1(t)]\cos(2n\cdot\omega_s t)\}\} \end{aligned} \tag{3}$$

where $J_k(x)$ is the 1st kind of Bessel function of order k, high-order harmonics can be ignored due to their negligible optical power, and we obtain

$$E_{out1} = 2E_0 \cos[\frac{\pi}{2}\alpha_2 D_2(t)]J_1[\frac{\pi}{2}\alpha_1 D_1(t)]\cos(\omega_c t)\cos(\omega_s t) - E_0 \sin[\frac{\pi}{2}\alpha_2 D_2(t)]J_0[\frac{\pi}{2}\alpha_1 D_1(t)]\cos(\omega_c t) \tag{4}$$

Since cos(x) and $J_0(x)$ are even functions, and sin(x) and $J_1(x)$ are odd functions, under the condition that $D_1(t)$ and $D_2(t)$ = [1 or −1], one can derive the Eq. (4) as

#167150 - $15.00 USD
Received 20 Apr 2012; accepted 7 May 2012; published 15 Jun 2012
(C) 2012 OSA

$$E_{out1} = E_0 \cos(\frac{\pi}{2}\alpha_2) J_1(\frac{\pi}{2}\alpha_1) D_1(t)\{\cos[(\omega_c+\omega_s)t]+\cos[(\omega_c-\omega_s)t]\} - E_0 \sin(\frac{\pi}{2}\alpha_2) D_2(t) J_0(\frac{\pi}{2}\alpha_1)\cos(\omega_c t)$$
$$= E_0 \cos(\frac{\pi}{2}\alpha_2) J_1(\frac{\pi}{2}\alpha_1)\{\cos[(\omega_c+\omega_s)t+\Phi_1(t)]+\cos[(\omega_c-\omega_s)t+\Phi_1(t)]\} - E_0 \sin(\frac{\pi}{2}\alpha_2) J_0(\frac{\pi}{2}\alpha_1)\cos[\omega_c t+\Phi_2(t)]\} \quad (5)$$

where $\Phi_1(t)$ and $\Phi_2(t)$ = [0 or π], representing the phase information of $D_1(t)$ and $D_2(t)$. We can adjust α_2 to satisfy the condition of $\cos(\frac{\pi}{2}\alpha_2) = \sin(\frac{\pi}{2}\alpha_2)$, then the Eq. (5) can be normalized as

$$E_{out1} \approx \{J_1(\frac{\pi}{2}\alpha_1)\cos[(\omega_c+\omega_s)t+\Phi_1(t)]+J_1(\frac{\pi}{2}\alpha_1)\cos[(\omega_c-\omega_s)t+\Phi_1(t)]\} - J_0(\frac{\pi}{2}\alpha_1)\cos[\omega_c t+\Phi_2(t)] \quad (6)$$

where the information of Data-1 and Data-2 are carried on the first-order and the baseband carries with DPSK modulation respectively, as represented by $\Phi_1(t)$ and $\Phi_2(t)$. The first-order of MZM-1 is then fed into the second modulator (MZM-2) driven by another RF clock S_{RF2}. The RF driver of MZM-2 together with the bias voltage can be described by $V_2(t) = \varepsilon_2 V_\pi + \alpha_{RF2} V_\pi \cos(\omega_s t+\beta)$, where ε_2, α_{RF2} are the bias voltage of MZM-2 and the driving amplitude of the RF clock S_{RF2} normalized to V_π. The output of MZM-2 can be expressed by

$$E_{out2} = E_0\{J_1(\frac{\pi}{2}\alpha_1)\cos[(\omega_c+\omega_s)t+\Phi_1(t)]+J_1(\frac{\pi}{2}\alpha_1)\cos[(\omega_c-\omega_s)t+\Phi_1(t)]\}\bullet\cos\{\frac{\pi}{2}[\varepsilon_2+\alpha_{RF2}\cos(\omega_s t+\beta)]\} \quad (7)$$

Since the MZM-2 is biased at the peak of transmission curve (ε_2 = 0), an expansion of the Eq. (7) with Bessel functions leads to an approximate expression for the output field as

$$E_{out2} = -E_0 J_1(\frac{\pi}{2}\alpha_1)\bullet\{J_0(\frac{\pi}{2}\alpha_{RF2})\cos[(\omega_c-\omega_s)t+\Phi_1(t)] - J_2(\frac{\pi}{2}\alpha_{RF2})\cos[(\omega_c-\omega_s)t+\Phi_1(t)-2\beta]\}$$
$$- E_0 J_1(\frac{\pi}{2}\alpha_1)\bullet\{J_0(\frac{\pi}{2}\alpha_{RF2})\cos[(\omega_c+\omega_s)t+\Phi_1(t)] - J_2(\frac{\pi}{2}\alpha_{RF2})\cos[(\omega_c+\omega_s)t+\Phi_1(t)+2\beta]\}$$
$$+ E_0 J_1(\frac{\pi}{2}\alpha_1)\bullet\{(J_2(\frac{\pi}{2}\alpha_{RF2})\cos[(\omega_c+3\omega_s)t+\Phi_1(t)+2\beta] + J_2(\frac{\pi}{2}\alpha_{RF2})\cos[(\omega_c-3\omega_s)t+\Phi_1(t)-2\beta]\} \quad (8)$$

where the higher order sidebands are ignored due to the small optical powers. Therefore, the output of MZM-2 consists of four frequency components ($\omega_c + \omega_s$, $\omega_c + 3\omega_s$). One can adjust the phase shifter (PS) and the RF amplifier to satisfy the conditions: $J_0(\alpha_{RF2}\pi/2) = J_2(\alpha_{RF2}\pi/2)$ and $\beta = 0$. In that case, only two tones of the highest and lowest frequencies remain, which are spaced by a six-fold frequency of the electrical driving signal and both carry the same DPSK information, while other components are greatly suppressed.

The schematic diagram of the proposed WDM-PON-RoF converged system is shown in Fig. 2. In the OLT/CS, for each WDM channel, wireless data (Data 1) is mixed with a 10-GHz RF clock to generate an electrical subcarrier multiplexed (SCM) signal, which is added with a wired data (Data 2) using a combiner. The output of the combiner is used to drive a single-drive MZM biased at the null point of the transmission curve. With this modulation, the wireless data (Data 1) is carried on the first-order sub-carriers in an OCS-DPSK format with 20-GHz repetition rate. The wired data (Data 2) is loaded on the baseband optical carrier in a DPSK format [15]. Through an array waveguide grating (AWG) or Nx1 optical coupler, the optical signals from all channels are combined and coupled into one fiber. An interleaver is used to separate the 20-GHz OCS-DPSK signals from the input signal. The 20-GHz OCS-DPSK signals of all the channels are then up-converted simultaneously using only one single-drive MZM, which is biased at the peak of the transmission curve and driven by a 10-GHz RF

#167150 - $15.00 USD Received 20 Apr 2012; accepted 7 May 2012; published 15 Jun 2012
(C) 2012 OSA

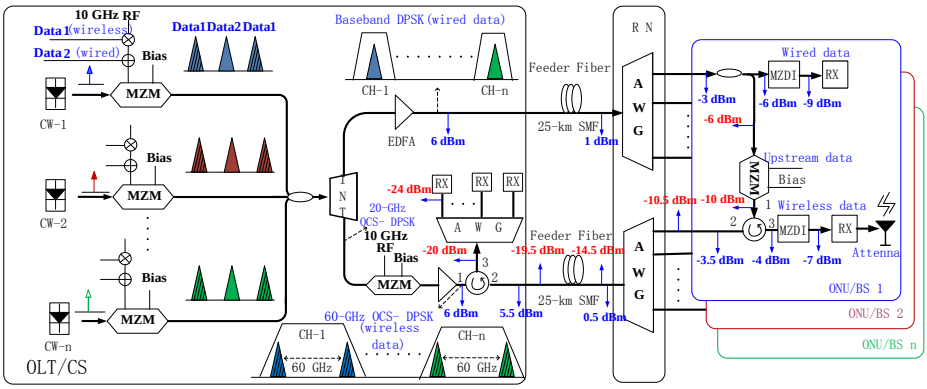

Fig. 2. Schematic diagram of the integrated WDM-PON-RoF system.

clock. In this manner, for all the WDM channels, 60-GHz OCS-DPSK signals can be achieved, which are transmitted to remote node (RN) through a 25-km standard single-mode fiber (SMF) shared by the upstream signals. After transmission, an AWG is employed to de-multiplex the 60-GHz OCS-DPSK signals and route them to the individual ONU/BS, where a high-speed OCS-DPSK receiver and an antenna are used to recover and broadcast the wireless data for wireless users. On the other hand, the baseband DPSK signals (wired data) are also transmitted to the RN for de-multiplexing and delivered into the corresponding ONU/BS. The baseband DPSK signal is detected with a low-speed DPSK receiver to recover the data for wired users. Part of the baseband DPSK signal is used as the carrier of upstream re-modulation, eliminating light sources and wavelengths management in the ONUs/BSs. The generated upstream data are transmitted back to the OLT/CS, where they are detected by low-speed photo-detectors (PDs). Using this design, one can simultaneously transmit multi-channel downstream wired, wireless, and upstream signals in a bidirectional WDM-PON-RoF system.

We also calculate the power budget for this proposed WDM-PON-RoF system. We assume that the total output power of the erbium-doped fiber amplifier (EDFA) is 18 dBm and there are 16 WDM channels in this network. Therefore, the power of the baseband DPSK and the 60-GHz OCS-DPSK signal for each channel is 6 dBm. Based on typical performances of commercial components [4], the losses of the 25-km SMF, optical circulator, MZM, AWG, 3-dB optical coupler and optical DPSK demodulator are set to 5 dB, 0.5 dB, 4 dB, 4 dB, 3 dB, and 3 dB, respectively. In Fig. 2, we mark the power in each location, and the powers of the received wired, wireless, and upstream data are –9 dBm, –7 dBm, and –24 dBm, respectively. If avalanche photodiode (APD) receivers were used with a sensitivity of –30 dBm for 1.25-Gb/s data, the power margins for the wired, wireless and upstream signals would be 21 dB, 23 dB, and 6 dB, respectively.

3. Experimental setup and results

We perform an experiment to verify the feasibility of the proposed scheme with a setup shown in Fig. 3, where all data are 1.25-Gbit/s pseudo-random bit sequence (PRBS) streams with a word length of 2^{31}-1, and all the RF clocks originate from a same RF synthesizer (Anritsu MG3694 B). In the OLT/CS, the optical carriers of channel-1 and channel-2 are CW lights from two tunable lasers (HP8168F and ILX 7900B) with wavelengths of 1557.80 nm and 1558.60 nm, respectively. CW-1 and CW-2 are fed into single-drive MZMs (JDSU OC-92) to generate baseband DPSK signals and 20-GHz OCS-DPSK signals [15]. The optical signals from channel-1 and channe-2 are combined using a 50:50 optical coupler (Fig. 4(a)). Two cascading fiber Bragg gratings (FBGs) are utilized to separate the baseband DPSK signals and the 20-GHz OCS-DPSK signals of channel-1 and channel-2, respectively (FBG 1: central wavelength at 1557.80 nm, 3-dB bandwidth of 0.104 nm, reflection ratio of 90%; FBG

#167150 - $15.00 USD
Received 20 Apr 2012; accepted 7 May 2012; published 15 Jun 2012
(C) 2012 OSA

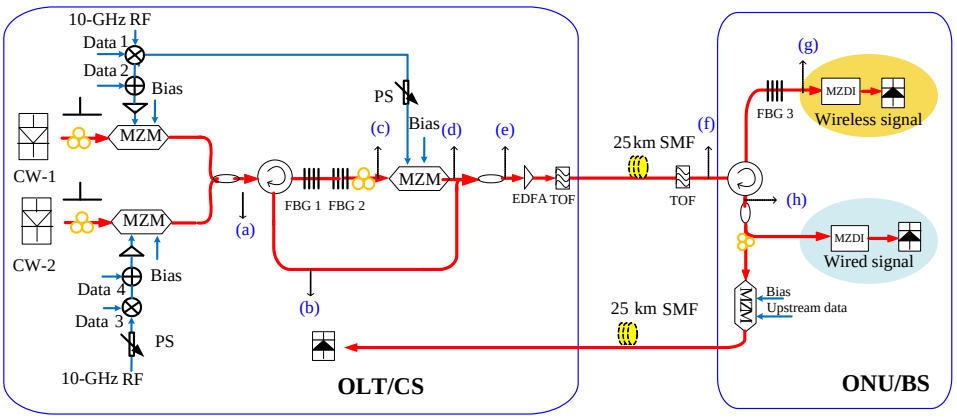

Fig. 3. Experimental setup of the proposed WDM-PON-RoF converged system. (a)–(h) correspond to the optical spectra shown in the Fig. 4.

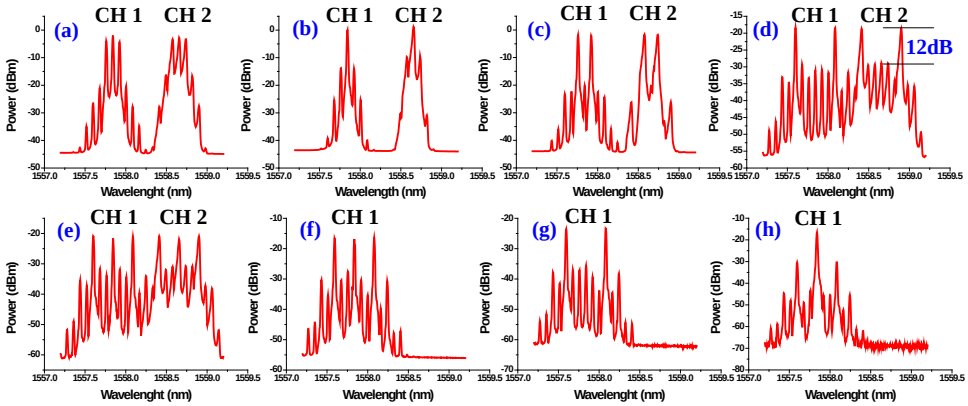

Fig. 4. Optical spectra taken at different positions as indicated in Fig. 3. Spectral resolution: 0.02 nm. (a) Baseband DPSK and 20-GHz OCS-DPSK signals, (b) reflected baseband signals, (c) passing signal from the cascading FBGs, (d) 60-GHz OCS-DPSK signals, (e) baseband DPSK and 60-GHz OCS-DPSK signals, (f) optical signal of channel-1, (g) 60-GHz OCS-DPSK signal of channel-1, (h) baseband signal of channel-1.

2: central wavelength at 1558.60 nm, 3-dB bandwidth of 0.106 nm, reflection ratio of 90%). When the number of channel increases, an interleaver is required to separate the baseband signals and the wireless signals, which go though the even and odd ports of the interleaver respectively. The passing 20-GHz OCS-DPSK signals (Fig. 4(c)) are up-converted using another single-drive MZM with a V_π of 6.7 V, which is biased at the peak of the transmission curve and driven by an amplified 10-GHz RF clock with a 13-V peak-to-peak voltage. The spectrum of the output of the MZM is shown in Fig. 4(d). It can be observed that the separation of the two tones of the OCS-DPSKs for both channels is 60 GHz (0.48 nm). As shown in Fig. 3, electrical phase shifters (PS) are used to control the delay between the two RF clocks, and polarization controllers (PC) are employed to control the polarization state of the input light fed into the MZMs. By modifying the PCs and PSs, more than 12-dB suppression ratio is obtained for the 60-GHz OCS-DPSK signals as shown in Fig. 4(d). Since only one high-performance filter (Alnair BVF 200) is available, the generated 60-GHz OCS-DPSK signals are combined with the baseband DPSK signals (Fig. 4(b)) using a 90:10 optical coupler and then amplified by an EDFA to a power of 6 dBm including both wired and wireless signals, which are transmitted through the same fiber and separated at the ONU/BS side. Better performances are expected in practical application (Fig. 2) as the signals would

#167150 - $15.00 USD
Received 20 Apr 2012; accepted 7 May 2012; published 15 Jun 2012
(C) 2012 OSA

experience less filtering effect and loss. A tunable optical filter (TOF) with a 3-dB bandwidth of 1.6 nm is utilized to suppress the amplified spontaneous noise (ASE) noise.

After transmission over 25-km SMF, the optical signal of channel-1 is selected using an optical filter with a tunable 3-dB bandwidth (Alnair BVF 200) and fed into the ONU/BS. Then the signal is separated by a FBG with a 3-dB bandwidth of 0.184 nm and a reflection ratio of 98%. The spectra of the passing signal (60-GHz OCS-DPSK signal) and the reflected signal (baseband DPSK signal) of the FBG are shown in Figs. 4(g) and 4(h). The optical eye diagram of 60-GHz OCS-DPSK signal is provided in Fig. 5(a), whose uneven envelope can be attributed to the limited bandwidth of oscilloscope (50 GHz). The envelope shows a periodicity of 800 ps, equaling to the period of one bit of the 1.25-Gb/s data. In real applications, in the ONU/BS, a diplexer connecting with an antenna would be used to broadcast the downstream wireless signal to the end users and a high-speed mixer would be employed to down-convert the upstream signal from the end users. In this particular demonstration, we mainly focus on the generation of 60-GHz MMW signals, and the signal is detected using a method similar to [14], where the bit-error-rate (BER) measurement is performed by detecting the upper-sideband component employing a low-speed receiver due to lack of high-speed PD and mixer. Simulations are carried out and similar BER results could be observed regardless of the detection methods [14]. On the other hand, the reflected baseband DPSK signal is split into two parts. The first one is received by a homemade DPSK receiver (8-GHz homemade Mach-Zehnder delay interferometer (MZDI) together with a low-speed PD) to recover the wired signal (Data 2), with its optical and electrical eye diagrams displayed in Figs. 5(c) and 5(d). Since the 1.25-Gb/s DPSK signal is de-modulated by the 8-GHz MZDI, the time delay between the two arms of the MZDI is less than one bit (5/32 bit) and the demodulated 1.25-Gb/s OOK is an RZ-like signal (Fig. 5(c)).The other part of DPSK signal is re-modulated by a MZM driven by the upstream data to achieve amplitude shift keying (ASK) modulation. As a result, the upstream signal is a ASK/DPSK orthogonal modulation format. The optical eye diagram of the ASK/DPSK signal is shown in Fig. 5(e), where the fluctuating ‘1’ level may originate from the remaining 60-GHz OCS-DPSK signal. In the OLT/CS, a 2.5-GHz receiver is used to detect the upstream ASK/DPSK signal and filter out the residual part of the high frequency signal, with an open eye diagram shown in Fig. 5(f). The PC in the ONU/BS is used to maintain good transmission performance, which can be eliminated if using commercially available polarization-insensitive modulators or reflective semiconductor optical amplifier (RSOA). In our experiment, a temperature controller (E-TEK MLDC-1016) is used to keep the temperature stable for the FBGs. The difference of the optical spectra for channel-1 and channel-2 in Fig. 4 could be attributed to the different performances of the components (lasers, modulator and electrical drivers etc.) used for the two channels.

The BER measurement results are provided in Fig. 6. For channel-1, after transmission of the 25-km SMF, error-free performance is obtained for the wireless data (60-GHz OCS-DPSK

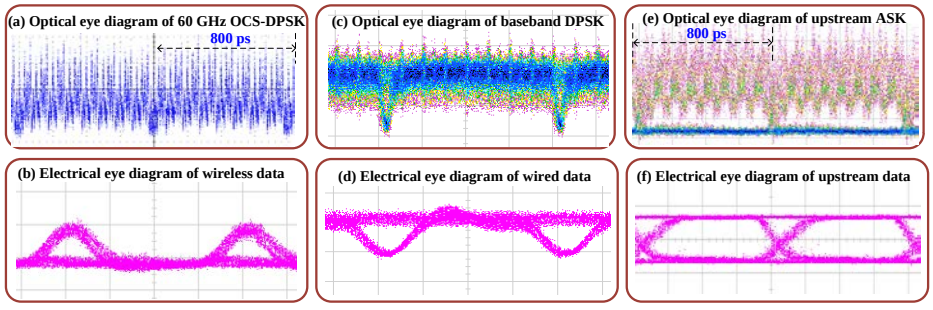

Fig. 5. Measured eye diagrams of downstream and upstream signals after transmission of 25-km SMF (X-axis: 200 ps/div).

#167150 - $15.00 USD Received 20 Apr 2012; accepted 7 May 2012; published 15 Jun 2012
(C) 2012 OSA

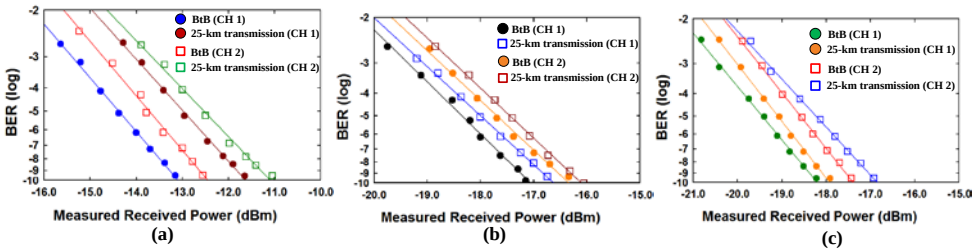

Fig. 6. BER curves of (a) downstream wireless data, (b) downstream wired data, (c) upstream re-modulation data.

signal) with 1.5-dB power penalty, which can be attributed to chromatic dispersion (CD) and imperfect filtering effect. While for the downstream wired (baseband DPSK signal) and upstream data (ASK signal), the power penalties are less than 0.5 dB. The BER performances of channel-2 are slightly worse than the ones of channel-1, which can be attributed to different performances of the components (lasers, modulators, electronic devices etc.) of the two channels. If balanced receivers were used, a 3-dB sensitivity improvement could be expected for the DPSK signals.

4. Conclusion

We have proposed a simple, cost-effective, and bi-directional WDM-PON-RoF converged architecture. The 60-GHz OCS-DPSK signals in two channels are experimentally demonstrated using only 10-GHz single-drive MZMs and 10-GHz RF components. Simultaneous generation and transmission of the 1.25-Gbps independent downstream wired and wireless signals are realized, with symmetric upstream data transmission over 25-km SMF. Error-free performances are achieved for all the data in both channels with less than 1.5-dB power penalties. The scheme can be scalable to N channels by using N + 1 modulators. The experimental results verify that our scheme could be a promising candidate for future wired and wireless converged networks.

Acknowledgments

This work was supported in part by NSFC (61077052/61125504), MoE (20110073110012), and Science and Technology Commission of Shanghai Municipality (11530700400).

#167150 - $15.00 USD Received 20 Apr 2012; accepted 7 May 2012; published 15 Jun 2012
(C) 2012 OSA